Journal of the Earth and Space Physics, Vol. 46, No. 4, Winter 2021, P. 65-77 (Research)

DOI: 10.22059/jesphys.2020.282486.1007124

A Semi-Automatic 2-D Linear Inversion Algorithm Including Depth Weighting Function for DC Resistivity Data: A Case Study on Archeological Data Sets of Pompeii

Varfinezhad, R.[1] and Oskooi, B.[2*]

1. Ph.D. Student, Department of Earth Physics, Institute of Geophysics, University of Tehran, Tehran, Iran
2. Associate Professor, Department of Earth Physics, Institute of Geophysics, University of Tehran, Tehran, Iran

(Received: 8 June 2019, Accepted: 21 Jan 2020)

Abstract

In this paper, a new simple, efficient and semi-automatic algorithm including depth weighting constraint is introduced for 2-D DC resistivity data inversion. Inversion procedure is linear; however, DC resistivity data inversion is generally nonlinear due to the nonlinearity of Maxwell's equation relative to resistivity (conductivity). We took the advantage of the 2-D forward operator formula obtained based on integral equations (IE) by Perez- Flores et al. (2001), for the inversion algorithm. Inversion algorithm is iterative and regularization parameter and depth weighting exponent are the critical parameters that have default values of 0.1 and 1, respectively. The presented technique was used only for dipole-dipole array by Perez-Flores et al. (2001), but here in addition to improving results for dipole-dipole array, its productivity is demonstrated for other geo-electrical arrays such as Wenner alfa, Wenner Schlumberger. Three synthetic data sets computed by Res2dmod software are utilized to investigate the performance of the algorithm through comparing the results with Res2dinv software output sections. Finally, the algorithm is applied on an archeological data set of Pompeii, which was collected by dipole-dipole array. IE inversion algorithm lead to satisfactory inversion models for both synthetic and real cases which reconstruct the subsurface better than or as well as that of the software.

Keywords: DC resistivity, Depth weighting, Integral equation, Inversion, Res2dinv.

1. Introduction

The direct current (DC) resistivity method is one of the most common methods for the exploration of the earth's subsurface due to being a cost-effective and well-established method (Wei et al., 2013). The purpose of electrical resistivity tomography (ERT) surveys is to determine the subsurface resistivity distribution both horizontally and vertically by making measurements on the ground surface. Introducing an efficient algorithm for inversion of resistivity data is necessary because quantitative interpretation cannot be made from the non-inversed data and interpretation based on pseudo-section is qualitative.

The DC resistivity quantitative interpretation has been developed largely over the years and various techniques have been proposed for DC resistivity inversion (e.g., Loke and Dahlin, 1997; Jackson et al., 2001; Pérez-Flores et al., 2001; Loke et al., 2003; Günther et al., 2006; Boonchaisuk et al., 2008; Li et al., 2012; Wei et al., 2013; Timothy et al., 2015). The numerical calculation of the electric field started in the late 1960s using the techniques of integral equations (Dieter et al., 1969), which is the case here, then other numerical techniques such as finite element (FE) (Coggon, 1971) and finite difference (FD) (Mufti, 1976) were introduced to DC resistivity forward modeling. The Integral Equation (IE) method is a powerful tool in electromagnetic (EM) modeling for geophysical applications especially for those models that have a background conductivity with simple structure (Zhadanov, 2009). The main advantage of the IE method in comparison with the FD and FE methods is the fast and accurate simulation of the response in models with compact 2-D or 3-D bodies in a layered background (Varfinezhad and Oskooi, 2019). Resistivity data inversion is generally nonlinear, but here, a linear method proposed by Perez-Flores et al. (2001) is used.

During the past few decades, there have been different algorithms for resistivity data inversion, most of which solved the problem in nonlinear form. General formula of their objective function is as follows:

*Corresponding author: boskooi@ut.ac.ir

$\min \rightarrow \|\boldsymbol{W}_d(\boldsymbol{F}(\boldsymbol{m})-\boldsymbol{d})\|_2^2+\alpha\|\boldsymbol{W}_m(\boldsymbol{m}-\boldsymbol{m}_0)\|_2^2$ where $\boldsymbol{d}$, $\mathbf{F}(\mathbf{m})$, $\mathbf{m_0}$ and m are observed data vector, calculated forward response, initial model and updated model obtained from adding updating term **dm** to $\mathbf{m_0}$; $\boldsymbol{W}_d$ and $\boldsymbol{W}_m$ are data and model weighting matrices and α is regularization parameter. Smith and Vozoff (1984) used just the first term without data weighting matrix and instead of the second term they used Truncated Singular Value Decomposition (TSVD) as another way of regularization. Narayan et. al (1994) used both terms but with some differences. Model weighting matrix is not used and regularization parameter adoption is different. Sasaki (1994) applied model weighting matrix, which was the second smoothness operator; Gunther et al. (2006) as well as Perez-Flores et al. (2001) utilized both data and model weighting matrices, which were data covariance matrix and smoothness operator, respectively. However, Perez-Flores et al. solved a linear problem that was based on integral equation. In addition to smoothness constraint. It can be said that these weights act as depth weighting function, but their mathematic formulas are not known. A 2-D inversion scheme with lateral constraint and sharp boundaries was introduced by Auken and Christiansen (2004). They believed that quasi-layered model can show actual geology more accurately in sedimentary environments. In general, the algorithm used by Loke and Barker it for RES2DINV software which is the most versatile one for different cases.

Depth weighting function introduced by Li and Oldenberg (1996 and 1998) for 3-D inversion of magnetic and gravity data that were utilized to compensate for the natural decay of the kernel matrix values with increasing depth. The exponent of this function generally depends on the depth of the anomaly; therefore, a reliable priori information about possible depth range of the anomaly is required. Li and Oldenberg (1996 and 1998) suggested exponent 2 and 3 for gravity and magnetic methods, respectively. In the absence of this, constraint cells that are near to the surface have larger weights in the inversion procedure. Depth weighting is going to be inserted into the inverse algorithm as weighting matrix with clear determination of its exponent.

In this paper, the 2-D formula of DC resistivity kernel obtained by Perez-Flores et al. (2001) is going to be manipulated, but they used it just for dipole-dipole array. Here we extend it for other geoelectric arrays. Weighted damped least-squares solution including depth weighting function as weighting matrix is adopted for inversion algorithm. Regularization parameter and the exponent of depth weighting are the critical parameters for this algorithm which are going to be addressed how to be determined. This technique is applied on different synthetic and real data sets and the results will be compared with Res2dinv software, which is the most widespread and standard software for 2-D DC resistivity data. Exact synthetic data are calculated by Res2dmod.

2. Methodology

2-1. 2-D forward operator

3-D formula of DC resistivity Kernel obtained by Perez-Flores et al. (2001) is as Equation (1):

$$\mathbf{K}_{\mathrm{DD}}=\mathrm{C}\sum_j\sum_i\left[\frac{(\mathbf{r}_C-\mathbf{r}_i)(\mathbf{r}_j-\mathbf{r}_C)}{|\mathbf{r}_C-\mathbf{r}_i|^3|\mathbf{r}_j-\mathbf{r}_C|^3}\right] \quad with \quad i=A.B \quad and \quad j=M.N$$

where

$$\mathrm{C}=\frac{-n(n+1)(n+2)a}{4\pi} \tag{1}$$

where $\mathbf{r}_C$, $\mathbf{r}_i$ and $\mathbf{r}_j$ are vectors defining coordinates of cell centers, current and potential electrodes, respectively, a is dipole separation and n is the values multiplied by dipole separation to increase the distance between current and potential electrodes in order investigate greater depths. Vectors $\mathbf{r}_C$, $\mathbf{r}_i$ and $\mathbf{r}_j$ are generally defined as:

$$\begin{aligned}\mathbf{r}_C&=x_c\mathbf{i}+y_c\mathbf{j}+z_c\mathbf{k}\\ \mathbf{r}_i&=x_i\mathbf{i}+y_i\mathbf{j}+z_i\mathbf{k}\\ \mathbf{r}_j&=x_j\mathbf{i}+y_j\mathbf{j}+z_j\mathbf{k}\end{aligned} \tag{2}$$

In fact, the integral form of the interested forward problem can be considered as a Fred-Holm Integral Equation of the first kind (IFKs). Integrating the Equation (1) in y direction from -∞ to ∞ leads to the 2-D form of IFKs (Varfinezhad and Oskooi, 2019):

$$d(s)=\int \boldsymbol{G}(s.x_c.z_c)\boldsymbol{m}(x_c.z_c)dxdz \tag{3}$$

where s represents current and potential

electrodes, d is the logarithm of apparent resistivity values, $(x_c. z_c)$ are coordinates of points of the interested area, $\boldsymbol{G}$ is kernel and $\boldsymbol{m}$ is the model.
Dividing the subsurface to $n_x \times n_z$ cells and discretizing the previous equation gives rise to the following matrix equation (Varfinezhad and Oskooi, 2019):

$$\boldsymbol{d} = \boldsymbol{Am} \quad (4)$$

where $\boldsymbol{A}$ is the 2-D forward operator, and readers are referred to the forward modeling paper by Varfinezhad and Oskooi (2019) for efficient calculation of forward operator.

2-2. Inversion algorithm

Solving Equation (4) in order to find the model parameters $\boldsymbol{m}$ is made by inversion. For an initial model $\boldsymbol{m_a}$ and from Equation (4), forward response is computed as:

$$\boldsymbol{Am_a} = \boldsymbol{d}_0 \quad (5)$$

Subtracting Equation (5) from (4), we have:

$$\boldsymbol{A}(\boldsymbol{m} - \boldsymbol{m_a}) = \boldsymbol{d} - \boldsymbol{d}_0$$
$$or \quad \boldsymbol{A}\Delta\boldsymbol{m} = \Delta\boldsymbol{d} \quad since \quad \Delta\boldsymbol{m} = \boldsymbol{m} - \boldsymbol{m_a}. \quad \Delta\boldsymbol{d} = \boldsymbol{d} - \boldsymbol{d}_0 \quad (6)$$

By multiplying $\boldsymbol{W_m A^T}$ on the both sides of Equation (6), Equation (7) is obtained:

$$\boldsymbol{W_m A^T A}(\boldsymbol{m} - \boldsymbol{m_a}) = \boldsymbol{W_m A^T}(\boldsymbol{d} - \boldsymbol{d}_0) \quad (7)$$

$\boldsymbol{W_m}$ is the weighting matrix.
Updated term $\Delta\boldsymbol{m} = \boldsymbol{m} - \boldsymbol{m_a}$ is calculated as:

$$(\boldsymbol{m} - \boldsymbol{m_a}) = (\boldsymbol{W_m A^T A})^{-1}(\boldsymbol{W_m A^T})(\boldsymbol{d} - \boldsymbol{d}_0) \quad (8)$$

Regularizing Equation (8) by taking advantage of the zeroth-order Tikhonov regularization technique leads to Equation (9):

$$\boldsymbol{m} = \boldsymbol{m_a} + (\boldsymbol{W_m A^T A} + \alpha^2 \boldsymbol{I})^{-1}(\boldsymbol{W_m A^T})(\boldsymbol{d} - \boldsymbol{Am_a}) \quad (9)$$

$\boldsymbol{I}$ and α are identity matrix and regularization parameter, respectively. $\boldsymbol{W_m}$ representing depth weighting matrix and is defined as:

$$\boldsymbol{W_m} = \frac{1}{\boldsymbol{z_c}^{\beta}} \quad (10)$$

where $\boldsymbol{z_c}$ is the z coordinates of cell centers and β is depth weighting exponent and we are trying to address how this to be chosen. The algorithm is started with an initial model $\boldsymbol{m_a}$ that assumed here to be a homogenous model with apparent resistivity equal to the background value of observed data, but it should be said that other initial models derived from any other geophysical methods or a priori information can also be used, which is not the case in both synthetic and real cases of this paper. Iterative inversion procedure stops after four iterations, and it rarely needs to be changed to the other values, but desired solution is always captured during 10 iterations. α and β are mostly constant values and only for some cases replacement of other values are required. These replacements are also very easy to be made as will be shown in the following sections. Ultimately, in addition to simplicity, effectiveness, the IE code is a semi-automatic code.

3. Synthetic models

Three different synthetic models are considered to investigate the efficiency of the suggested technique, and Res2dmod software is used for calculating model forward responses to produce exact synthetic data. Inversion result derived from the IE technique are compared with the results of Res2dinv software to demonstrate its productivity. Res2dinv results are shown in MATLAB to have an identical representation system for both methods and comparisons can be made better. For all cases, if the profile length is L, and a is the smallest electrode spacing, then the number of cells in x and z directions (n_x, n_z) and the cell lengths l_x and l_z are determined as $n_x=L/a$, $n_z=L/(4a)$ and $l_x=l_z=a$.

3-1. Four conductive anomalies (Dipole-Dipole array)

First, the synthetic model is composed of four conductive anomalies with the same resistivity value of 20 Ω.m surrounded by a homogenous background with resistivity 100

Ω.m (see Figure 1). Dipole-dipole array with dipole separation of 10 m was used to calculate synthetic data and the computed apparent resistivities are made for n from 1 to 9. It should be mentioned that the forward modeling of this case using linear integral equation was made by Varfinezhad and Oskooi (2019) and the result is compared with that of Res2dmod software for which RMS value was 7.5%. Here our concentration is on inversion of exact data using linear integral equation to investigate its productivity. Retrieved models by the algorithm, Res2dinv and Perez-Flores et al. (2001) technique are shown in Figure 2. Comparing the results is suggestive of presented algorithm productivity and it can be asserted that its result is somewhat better than Res2dinv. It can also be observed that the inversion model obtained from the algorithm is significantly superior to the reconstructed model derived by Perez-Flores et al. Regularization parameter, depth weighting exponent and number of iterations are 0.1, 1 and 4, respectively. For most synthetic and real cases, these values are constant, and they need to be changed rarely. Therefore, these values can be chosen as default values for inverse procedure and inversion algorithm is a semi-automatic one. Two notes are suggested for changing default values: (i) if you think your recovered model is noisy, 0.5 can be considered for regularization parameter (ii) if you expect to see anomaly (anomalies) in less depth (depths) or subsurface is layered earth, 0.5 is suggested for the exponent of depth weighting function. RMS error values of the forward responses computed from IE algorithm and Res2dinv are 4.6% and 5.1%, respectively.

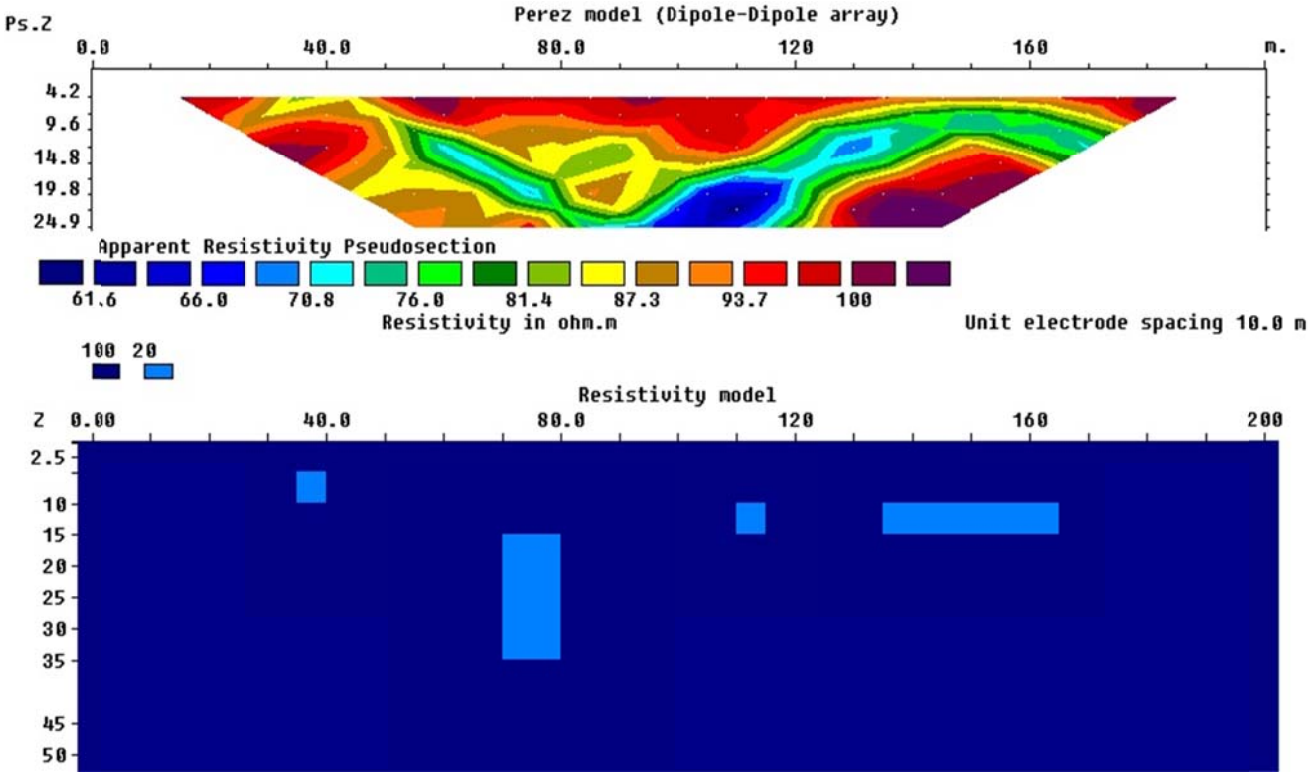

Figure 1. Four conductive anomalies surrounded by a resistive homogenous medium (top) and its forward response (bottom) calculated by RES2DMOD software.

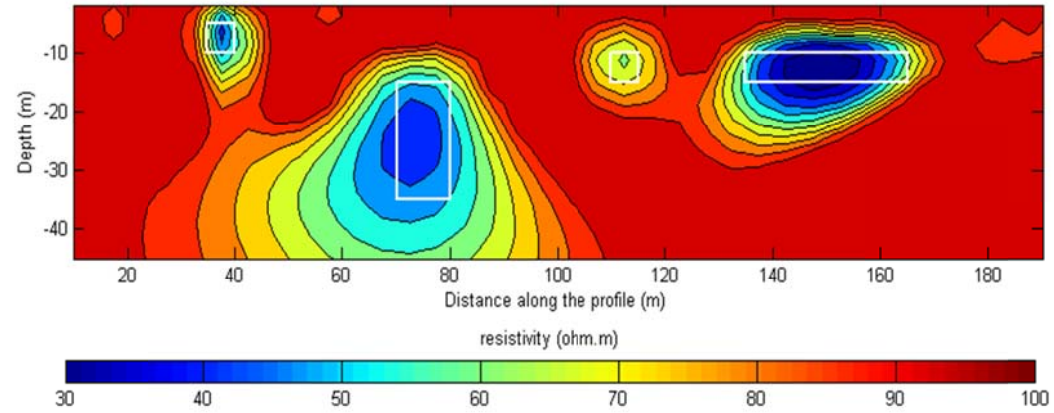

(a)

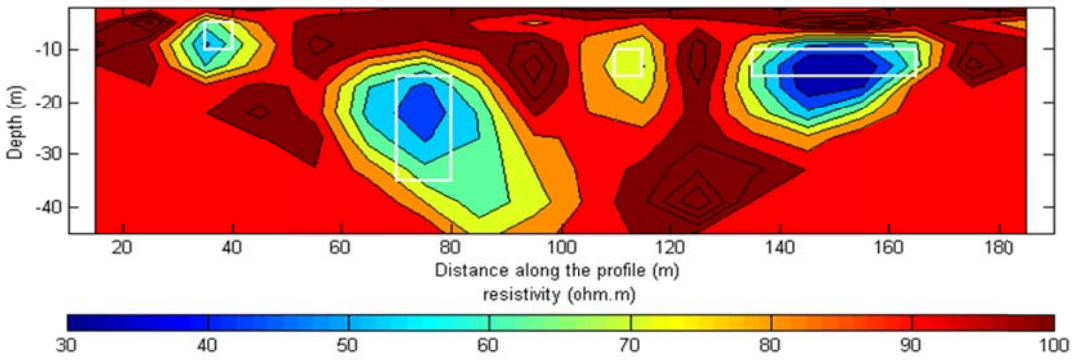

(b)

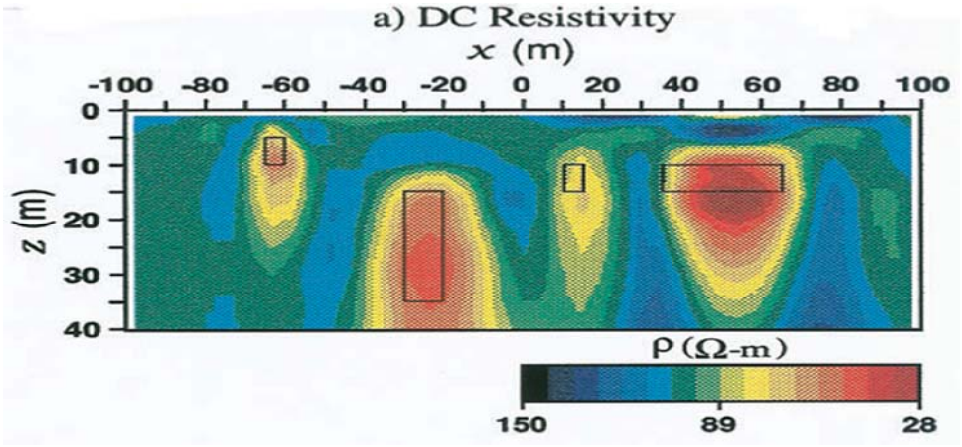

(c)

Figure 2. Reconstructed model derived by (a) IE code (b) Res2dinv software and (c) Perez-Flores et al. (2001). RMS error values of the forward responses computed from IE algorithm and Res2dinv are 4.6% and 5.1%, respectively.

3-2. block and dykes (Wenner Alfa)

The second synthetic case is a model of 12 blocks and dykes with different sizes and depths immersed in a homogeneous background with resistivity 1 Ω.m. The interested blocks and dyke resistivity values are 5 or 25 Ω.m. Wenner alfa array with unit electrode spacing is used for this complicated model. Figure 3 shows the synthetic model and computed data by Res2dmod software. Inverting synthetic data with IE code and inverse software leads to the results represented in Figure 4. Both methods recover 10 from 12 anomalies

and the first two blocks close to the start of the profile and thick dykes located at 40 and 48 m are retrieved as one anomaly because all of them are resistive relative to the background, and their effects are mixed with each other. It should be noted that, however, the two thick dykes are enough separated from each other, in contrast to the first two blocks, but their discriminations are not made because (i) penetrating to deeper depths demands the increase of electrode separations and consequently losing lateral resolution, and (ii) deeper dyke is less resistive despite its more thickness. Therefore, recovered anomaly is much more correlated with dykes positioned at 40 m and the dyke located at 48 m made the retrieved anomaly to be as an inclined one. This result can be seen well in IE inversion section. Comparing both IE and Res2dinv results is generally indicative of more resolved subsurface section derived by IE code. It can be asserted that the dyke place at 8 m and the small block at 20 m are the only anomalies retrieved better by the software and its advantage is related to its better depth extension recovery and clearer anomaly for the dyke and block, respectively. Default values of 0.1, 1 and 4 were chosen for regularization parameter, depth weighting exponent and number of iteration, respectively.

3-3. Fault and block (Wenner-Schlumberger)

The last considered numerical example is the model of fault and block using Wenner-Schlumberger array (Figure 5). Fault is made up of two areas with resistivity values of 10 and 40 Ω.m, and the block resistivity was considered to be 1 Ω.m. Depth to the top of both of them are assumed to be 0.75 m, and horizontal ranges of fault and block are from 0 to 17 and 24 to 26, respectively. Vertical extension of block is to 1.8 m, while fault is continued to the end of the area. Data are computed with 10 electrode spacing from 1 to 10 m. Figure 6 demonstrates the inversion section obtained by IE code and Res2dinv software. Horizontal position of the fault vertical boundary retrieved by IE code and software are close to 17 m (horizontal position of vertical boundary of the true fault), but recovered boundary by IE code is clearer than the software, while left side of it is recovered better by the software. Depth to top of the fault obtained by IE code and the software are close to 1 and 1.5 m, respectively, indicating better reconstruction by IE code; however, the transition area is smoothly changing especially for Res2dinv model. Comparing blocks in both inversion images with true block is demonstrative of well recovery of depth to top of the anomaly and horizontal position and extension obtained by both methods but vertical extension of the block derived by IE code is in more correspondence with the true one than the block reconstructed by the software. RMS error values of the forward responses derived from inversion solutions by IE and software are 3.5% and 3.8%, respectively, expressing insignificant difference between two methods and it is consistent with relative better result draw out from IE inversion algorithm.

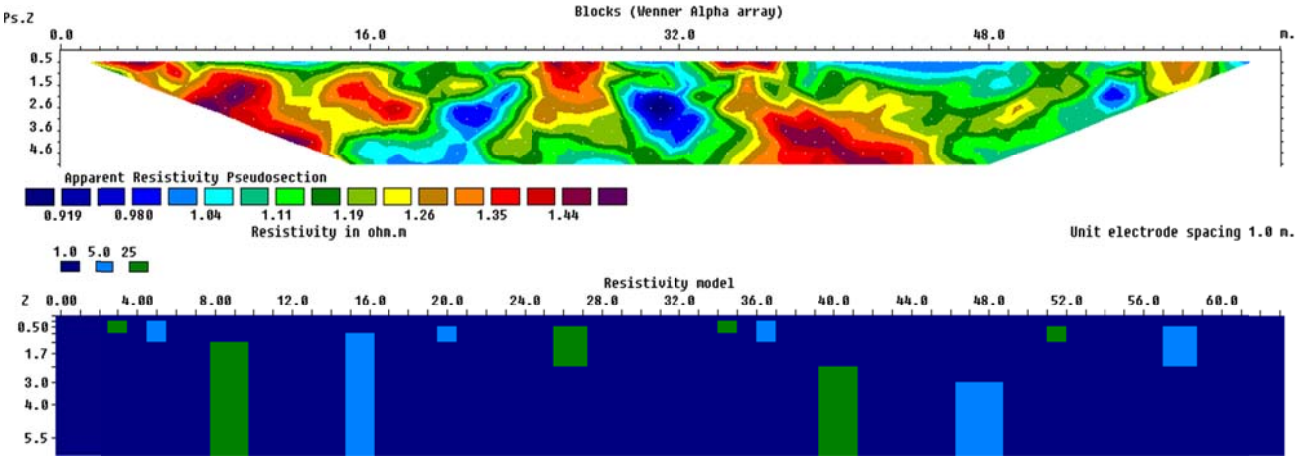

Figure 3. True model of some blocks and dykes in a uniform background and its pseudo-section for Wenner Alfa array.

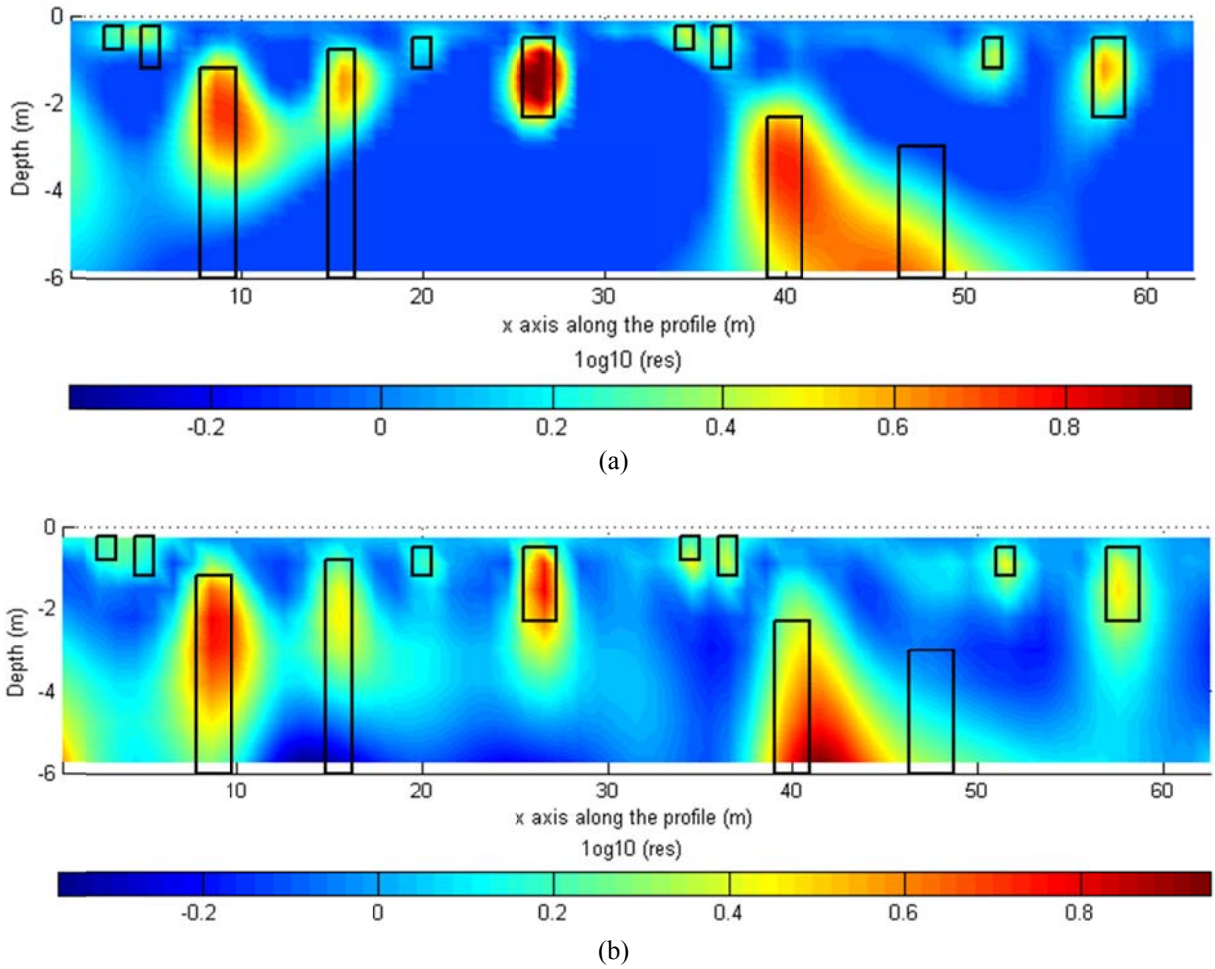

Figure 4. Retrieved models obtained by (a) IE code, (b) RES2DINV software.

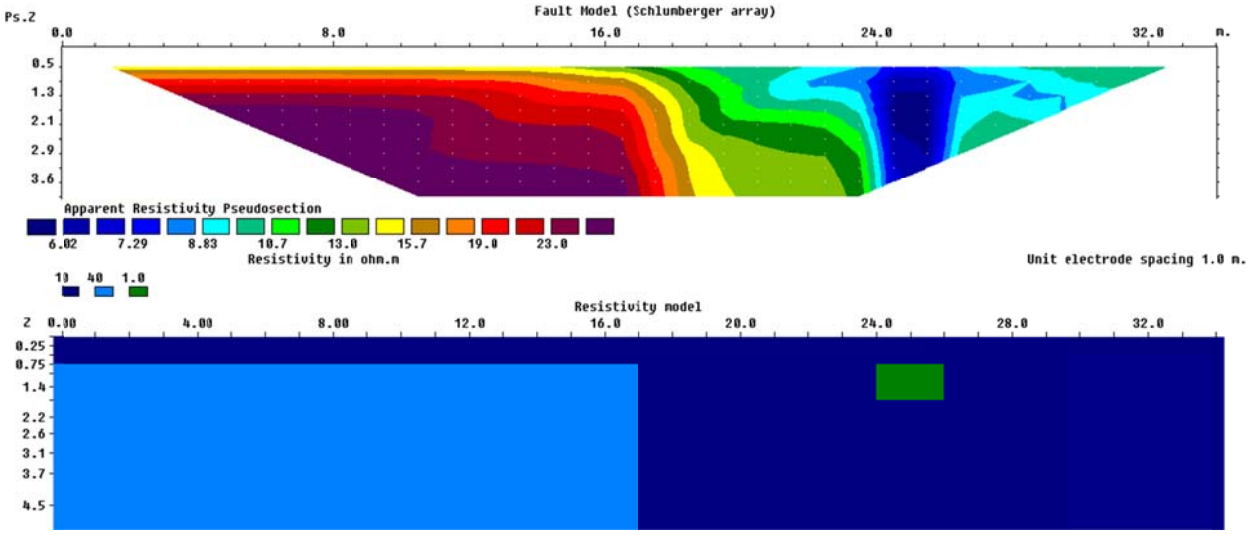

Figure 5. Fault and block model and its forward response for Wenner-Schlumberger calculated by RES2DMOD.

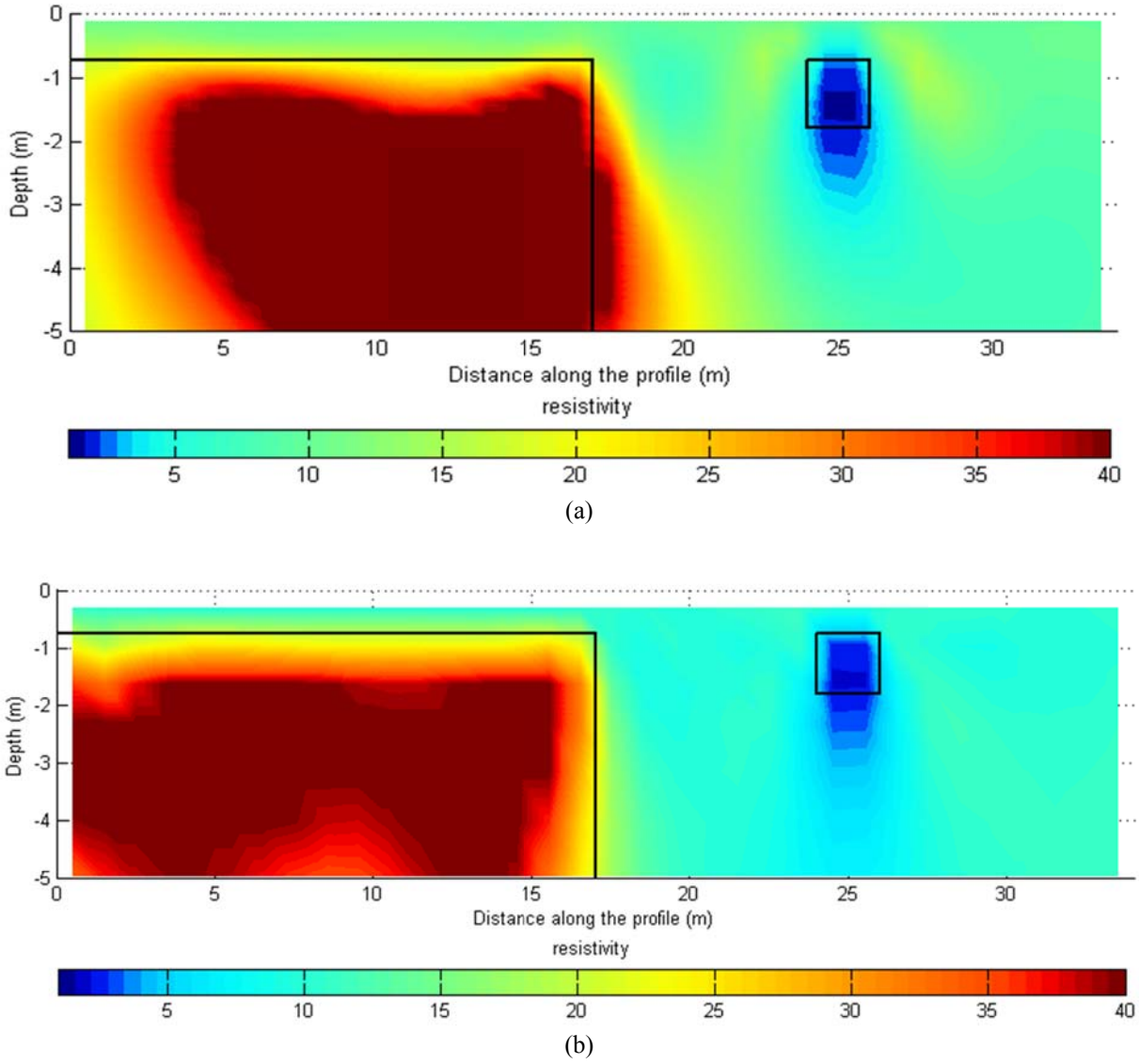

Figure 6. Inversion model attained from (a) IE, (b) RES2DINV software.

4. Discussion

In this section, we are going to examine the effect of depth weighting exponent and noise on IE algorithm and it will be demonstrated that why: i) depth weighting exponent is chosen to be 1, ii) regularization parameter can be increased to 0.5 for noisy data; however, it should be generally selected depending on the noise level. We know noise level in the synthetic cases but complexity of the interested model is also important. Here, we want to show that for a relatively complex model and for Gaussian noise with the level of 5% and 7.5%, 0.5 is a good choice. First synthetic case (Perez-Flores model) is adopted for this examination; however, the same can be done for others.

4-1 Depth weighting effect

At first, the effect of depth weighting exponent on inversion result of IE algorithm is investigated, while other inverse parameters are fixed (regularization parameter and number of iterations are assumed to 0.1 and 4, respectively). Figure 7 shows the inversion results for exponent values of 0, 0.5, 1 and 1.5 and two important conclusions can be made from this figures: I) increasing depth weighting exponent leads to recovering anomalies in deeper depths and as we suggested 1 is a good choice. In other two synthetic cases, it was shown that exponent

equal 1 results in satisfying retrieved sections, II) increasing depth weighting produces more resolved models and for higher values than 1 this increased resolution is at the cost of losing stability of the solution. In other words, depth weighting function has a contribution in regularization term so that the larger exponent value leads to more resolved but more unstable solution. The same occurs when we use small values for regularization parameter. These changes in reconstructed models due to the presence of depth weighting function can be justified according to Equation (10). W_m is a diagonal matrice and after multiplication by $A^T A$ it changes only the diagonal elements of $A^T A$ which is the same that is done by regularization parameter in terms of regularization term.

First, real case shows that 0.5 for layered case is an appropriate choice and demonstrating the proper exponent of 1 for non-layered mediums will be made by the second real data set.

4-2 Noise effect and choosing regularization parameter

Now, the effect of noise on IE inversion algorithm and adopting regularization parameter are probed. Gaussian noise with two levels 5% and 7.5 % of maximum value of data were added to the data, and we increased regularization parameter from 0.05 to 1.5. Figure 8(a-e) presents the reconstructed models from 5% noisy data for regularization parameters of 0.05, 0.1, 0.5, 1 and 1.5, respectively. Increasing regularization parameter solves the problem of instability of the inverse solution but resolution is limited as we expect, and considering trade-off between resolution and stability of the solution result in choosing 0.5 as a desired value for regularization parameter. Augmentation of noise level to 7.5% make inverse solution more unstable and the same procedure are repeated for mentioned regularization parameter values (Figure 8(f-j)), and our optimal value can be 0.5. Therefore, 0.5 can be a good choice for noisy data at these levels considered here, which are logical levels for many data sets, but for less noisy data smaller values and for noisier data larger values must be used. It should be said that relatively high level of noise (7.5%) was considered for a relatively complicated model, and we should take into account that we are using a linear operator. Considering the difference between computed data by exact method, using finite-difference or finite-element numerical techniques in nonlinear form or this linear method, by adding this level of noise, we can say that this simple algorithm is an efficient enough technique to be used for inverting DC resistivity data.

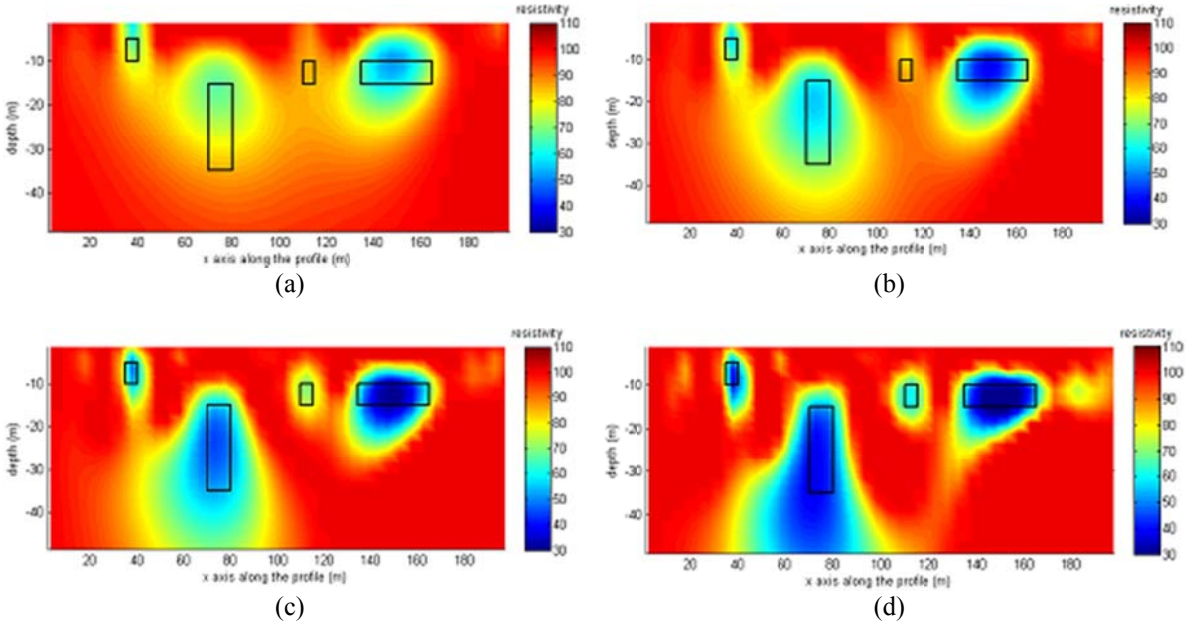

Figure 7. Inversion model derived from IE algorithm for depth weighting exponent values of (a) 0, (b) 0.5, (c) 1 and (d) 1.5.

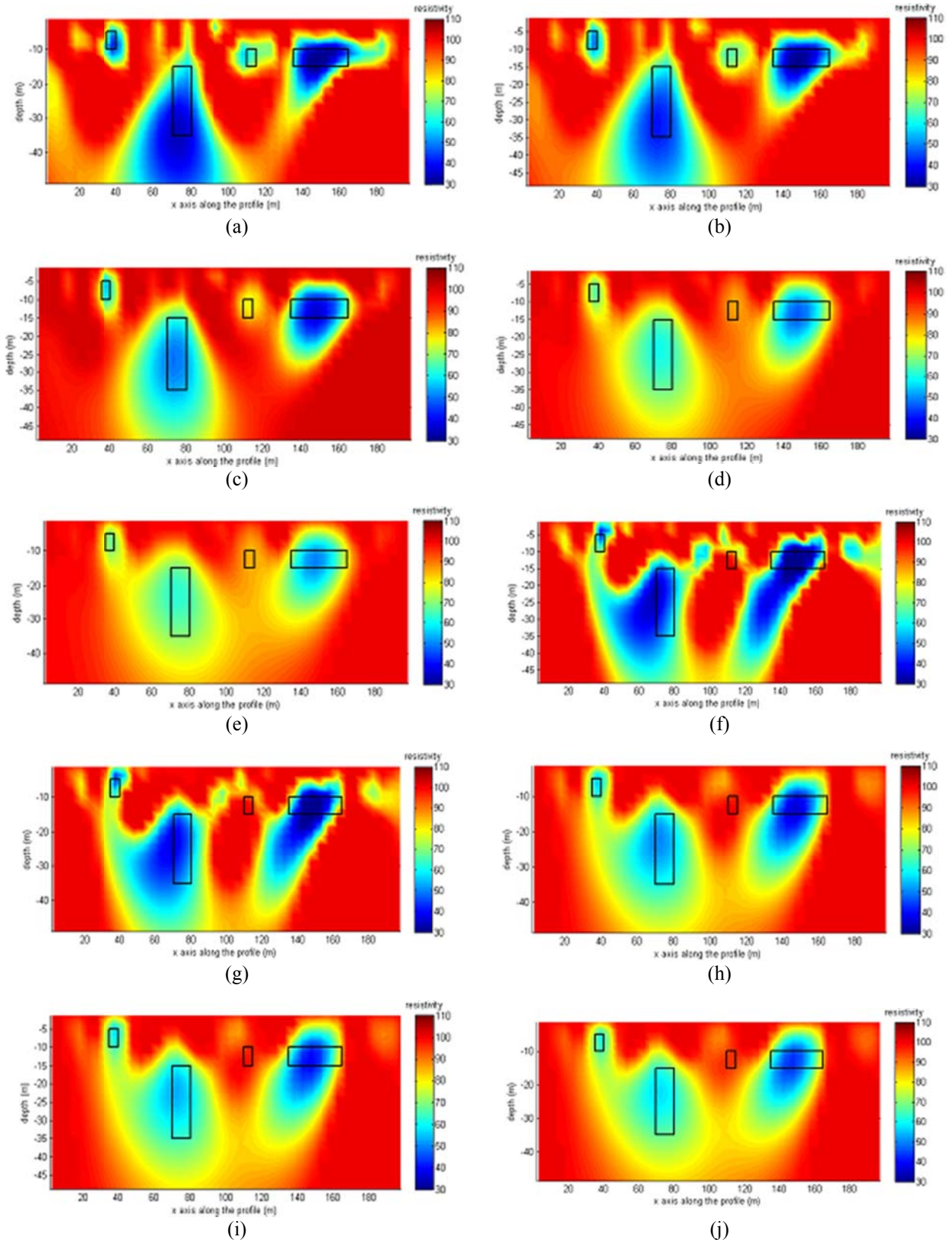

Figure 8. Inversion model derived from IE algorithm for noisy data: (a) noise level=5% regularization parameter=0.05, (b) noise level=5% regularization parameter=0.1, (c) noise level=5% regularization parameter=0.5, (d) noise level=5% regularization parameter=1, (e) noise level=5% regularization parameter=1.5, (f) noise level=7.5% regularization parameter=0.05, (g) noise level=7.5% regularization parameter=0.1, (h) noise level=7.5% regularization parameter=0.5, (i) noise level=7.5% regularization parameter=1 and (j) noise level=7.5% regularization parameter=1.5.

5. Real data: Archeological data (dipole-dipole)

Resistivity data set of a profile in the archeological area of Pompeii are used as the second real case to examine the performance of the this IE code. Resistivity profile is 35.5 m. Apparent resistivity data are collected by dipole-dipole array with three different dipole separations of 0.5, 1 and 2 m, which satisfies the required resolution and depth of exploration for the case. Number of the acquired apparent resistivity data for this profile is 597. Positions of the underground walls and the adopted profile can be observed in the map shown in Figure 9. The subsurface is discretized into 71 by 8 regular square cells in x and z directions, respectively, with the length of 0.5 m. The process is started with the homogenous models with the background value of 50 Ω.m. Regularization parameter and depth weighting exponent are chosen based on the mentioned experimental method and their fixed values are 0.1 and 1, respectively. Resistivity retrieved models by IE code and Res2dinv are presented in Figure 10, and wall positions are plotted on both figures. RMS error values are 3.6% and 4.7% for computed data from the IE and Res2dinv inversion models, respectively, indicating better fit of the computed data from IE result. According to the map, wall positions are at the distances 9, 12, 16, 18, 29, 31 and 34 m from the start of the profile. Recovered anomaly centers by IE code are at 2, 7, 9, 12.5, 15.5, 18, 25 and 34 m. Except the first and second anomalies which are not related to the walls, all other wall positions are in very good agreement with real positions of the walls, but it should be said that we lost the wall at 31 m, and the first and fifth walls situated at 8 and 29 m are not retrieved as clear as other walls. Res2dinv results consist of four major anomalies. First one with the center at 5 m elongated to 7 m, because maybe the effect of the first anomaly, which cannot be a wall, is mixed with the first wall at 8 m. Second anomaly starts after 10 m and continue to 15 m indicative of walls at 12 and 15, which are not differentiated from each other. Third one with the center at 18 m is exactly recovering wall at this position. Finally, the last anomaly from 29 to 35 m is representing the walls at 29, 31 and 34, which are also not discriminated. It can be concluded that IE code result retrieves the walls with more resolution than Res2dinv software; however, the inverse procedure used for the code is relatively an uncomplicated semi-automatic algorithm.

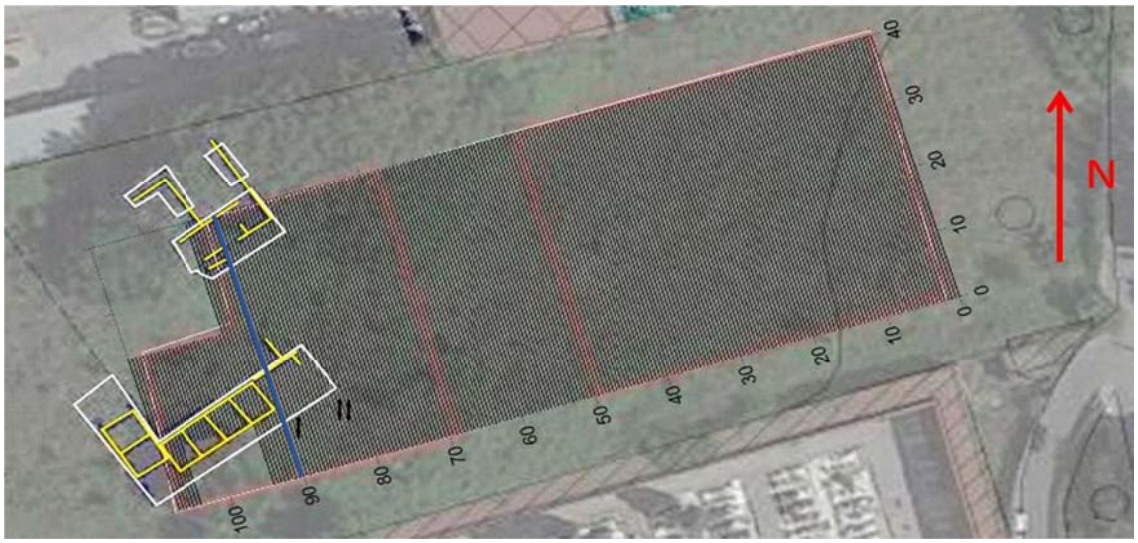

Figure 9. Map of the area. Blue line is the survey profile.

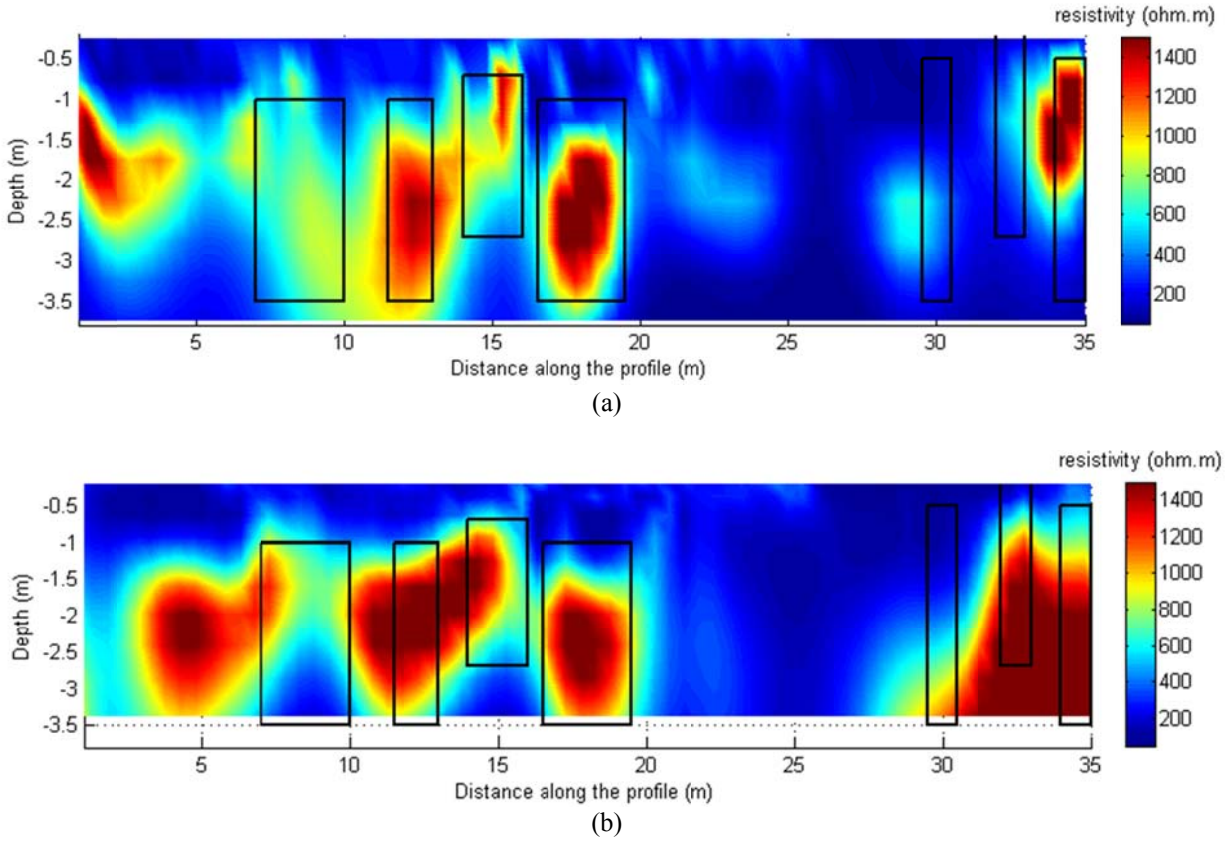

Figure 10. Inversion model derived by (a) IE code, (b) Res2dinv. RMS errors of IE and Res2dinv are 3.6 % and 4.7%, respectively.

6. Conclusion

A linear semi-automatic inversion algorithm including depth weighting function was introduced for 2-D DC resistivity data inversion around the axis of the formula extracted by Perez-Flores et al., for the 2-D linear forward operator of dipole-dipole array. The algorithm has four parameters: resistivity of homogeneous initial model that is equal to the background value of the measured data, number of iterations, regularization parameter and depth weighting exponent for which default values are 4, 0.1 and 1, respectively. For most cases, adopting these values leads to a desired inversion model. For the depth weighting function 0.5 is the only replacement value used when the medium is layered or we know from a priori information that the exponent equal to 1 produce anomaly or anomalies deeper than what they must be. The efficiency of the IE inversion algorithm was examined by applying it on synthetic and real data sets. Exact synthetic apparent resistivities for the three considered synthetic models were calculated by Res2dmod software. Three synthetic cases were considered: I) four conductive blocks immersed in a homogenous background using dipole-dipole array, II) block and dykes using Wenner alfa array, and III) fault and block model for Wenner-Schlumberger array. For the real case, an archeological data sets of a region in Pompeii was utilized. The performance of the algorithm on these synthetic and real cases were investigated and the results were compared with corresponding Res2dinv inversion sections. Generally speaking, IE inversion algorithm results were superior to their counterparts derived by Res2dinv.

References

Auken, E. and Christiansen, A. V., 2004, Layered and laterally constrained 2D inversion of resistivity data, Geophysics, 69(3), 752–761.

Boonchaisuk, S., Vachiratienchai, C. and Siripunvaraporn, W., 2008, Two-dimensional direct current (DC) resistivity inversion: data space Occam's approach, *Phys.* Earth Planet. Inter, 168, 204–211.

Cockett, R., 1971, Direct Current Resistivity

Inversion using Various Objective Functions.

Coggon, J.H., Electromagnetic and electrical modelling by the finite element method, Geophysics, 36, 132–155.

Dieter, K., Paterson, N.R. and Grant, F.S., 1969, IP and resistivity type curves for three-dimensional bodies, Geophysics, 34, 615–632.

Günther, T., Rücker, C. and Spitzer, K., 2006, Three-dimensional modelling and inversion of DC resistivity data incorporating topography—II. Inversion, Geophysical Journal International, 166, 506-17.

Jackson, P.D., Earl, S.J. and Reece, G.J., 2001, 3D resistivity inversion using 2D measurements of the electric field, Geophysical Prospecting, 49, 26-39.

Li, C.W., Bin X., Qiang, J.K. and Lü, Y.Z., 2012, Multiple linear system techniques for 3D finite element method modeling of direct current resistivity, Journal of Central South University, 19, 424-32.

Li, Y. and Oldenburg, D. W, 1996, 3-D inversion of magnetic data, Geophysics, 61, 394-408.

Li, Y. and Oldenburg, D. W., 1998, 3D inversion of gravity data, Geophysics, 63, 109-19.

Loke, M.H., Acworth, R. and Dahlin, T., 2003, A comparison of smooth and blocky inversion methods in 2D electrical imaging surveys, Exploration Geophysics, 34(1), 182-87.

Loke, M.H. and Dahlin, T., 1997, A combined Gauss-Newton and Quasi-Newton inversion method for the interpretation of apparent resistivity pseudo-sections, In 3rd EEGS Meeting,

Mufti, I.R., 1976, Finite-difference resistivity modeling for arbitrarily shaped two-dimensional structures, Geophysics, 41, 62–78.

Narayan, S., Dusseault, M.B. and Nobes, D.C., 1994, Inversion techniques applied to resistivity inverse problems, Inverse Problems, 10(3), 669-686."

Perez-Flores, M.A., Méndez-Delgado S. and Gomez-Treviño, E., 2001, Imaging low frequency and dc electromagnetic fields using a simple linear approximation. Geophysics, 66, 1067–1081.

Sasaki, Y., 1994, 3D resistivity inversion using the finite-element method, Geophysics, 59, 1839–1848.

Smith, N.C. and Vozoff, K., 1984, Two dimensional DC resistivity inversion for dipole-dipole data, IEEE Trans. Gemeience Remote Sensing, 22, 21-28.

Timothy, W., Greenhalgh, S., Zhou, B., Greenhalgh, M. and Marescot, L., 2015, Resistivity inversion in 2-D anisotropic media: numerical experiments, Geophysical Journal International, 201, 247-66.

Varfinezhad, R. and Oskooi, B., 2019, 2D DC resistivity forward modeling based on the integral equation method and a comparison with the RES2DMOD results, Journal of Earth and Space Physics. doi:10.22059/jesphys. 2019.260824. 1007020.

Wei, W., Wu, X., and Spitzer, K., 2013, Three-dimensional DC anisotropic resistivity modelling using finite elements on unstructured grids, Geophysical Journal International, 193, 734-746.

Zhdanov, M.S., 2009, Geophysical electromagnetic theory and methods, Elsevier.